

Measurement of Auroral Characteristics by Auroral Turbulence II Sounding Rocket

M.A. Danielides¹, A. Ranta², N. Ivchenko³, J. Jussila¹, G. Marklund³ and F. Primdahl⁴

¹ Oulu University, Department of Physical Sciences, P.O. Box 3000, FIN-90401 Oulu, Finland

² Sodankylä Geophysical Observatory, FIN-99660 Sodankylä, Finland

³ Alfvén Laboratory, Royal Institute of Technology, Stockholm, Sweden

⁴ Danish Space Research Institute/Department of Automation, 327, Technical University of Denmark,
DK-2800 Lyngby, Denmark

(Received: December 1998; Accepted: March 1999)

Abstract

The Auroral Turbulence II sounding rocket was launched into a moderately active night-side aurora from the Poker Flat Research Range, Alaska, US. This unique three payload rocket experiment contained both electric and magnetic field, and particle instruments, which provided three point measurements over a wide range of scales. The payloads passed through several auroral arcs providing details of the auroral fine structure and the three point measurements allowed the distinction of spatial and temporal variations. The rocket data are compared with optical observations with special emphasis on a large quiet arc traversed in the middle of the flight. The observed features and field-aligned current densities are found to agree with earlier studies.

Key words:

1. Introduction

One primary goal of rocket born in-situ experiments in the Earth upper atmosphere is to study correlations between particles, magnetic and electric fields in auroral structures (Lühr, 1992, Primdahl *et al.*, 1979). Numerous rocket investigations of auroral arc electrodynamics have been performed during the last three decades (Evans *et al.*, 1977, Marklund *et al.*, 1982, Marklund, 1984). For a majority of these investigations single payloads were used with very limited possibilities for distinction between spatial and temporal variations. Johnstone and Davies (1974) reported two-point measurements of breakup aurora using a mother-daughter payload combination. Here we report on the first successful three-payload auroral experiment. The Auroral Turbulence II sounding rocket (AT-II) was launched from the Poker Flat Research Range near Fairbanks, Alaska, US at 08:36 UT on February 11 1997, under no moonlight conditions. It carried three payloads, North, East and Main payload, into the

upper atmosphere, to a maximum height of 500 km. The payloads were each equipped with a high-sensitivity magnetometer (*Primdahl et al.*, 1994) and particle, wave and electric field instruments. Several distinct auroral arc structures were crossed during the flight. Ground based optical observations were made at three places along the rocket trajectory, at Poker Flat, Fort Yukon and Kaktovik. A large-scale view of the auroral situation during the rocket flight was obtained by the POLAR satellite Ultraviolet Imager (UVI). In addition magnetic data from Poker Flat and GOES9 and Wind satellites were used.

2. *Rocket instrumentation*

Each of the three payloads were equipped with a vector electric field instrument (Cornell University, New Hampshire University (UNH), Dartmouth College), ion and electron mass-spectrometers (UNH) and a 3-component fluxgate magnetometer. The resolution of the magnetometer is 0.11 nT/bit for the North and East payloads, and 0.15 nT/bit for the Main payload (*Primdahl et al.*, 1994). The instrument was developed and constructed in collaboration between Technical University of Denmark (DTU), Terma Electronics A/S, Denmark, Royal Institute of Technology (RIT) and Sodankylä Geophysical Observatory (SGO). The magnetometer provided measurements of the B-field with a sampling rate of 2.0 kHz. The Main payload carried in addition several other instruments: two different wave-particle correlators and the Plasma Frequency Tracker both for measurements of waves and particles near the plasma and upper hybrid wave frequency. The electric field probes allowed high frequency sampling up to 6 MHz. The UNH Burst computer was programmed, similar to earlier missions (e.g. Greenland II and Auroral Turbulence I), to enable fast detection of changes in the particle precipitation pattern. The ambient electron density was measured by the Plasma Frequency Probe (Dartmouth). The magnetometer used is a new type of digital fluxgate instrument (*Primdahl et al.*, 1994), where the normal analog electronics were replaced by algorithms implemented in a Digital Signal Processor (DSP). The principle of operation is the same as in a normal analog fluxgate magnetometer, which is to generate a nulling signal to the sensor to compensate the external field.

The North and East payload were each ejected from the Mother payload at about 10 m/sec separation speed and at an angle of 45 degrees with respect to the B-field. Thus, a triangle of observation points was provided, the sides of the triangle expanding from 0 to 6 km during the flight, both perpendicular and parallel to the B-field.

3. *Measurements*

3.1 *Optical observations*

During the rocket flight optical observations were made by all-sky cameras at three places in Alaska, at Poker Flat, Fort Yukon and Kaktovik, and by UV-imager

(*Torr, 1995*) on the POLAR satellite. In Figure 1 the auroral situation seen by the POLAR UV-imager is shown for the time of the rocket flight above Alaska. The three optical ground stations and the coastline of Alaska are shown representing the geographic reference. The rocket trajectory along about 213° E longitude and payload cluster position are also marked. The different intensity levels in Figure 1a and 1b are caused by the two different filters used in the UV-imager (*Zukic, 1993*). The filter design results in a significant reduction of the visible light while maintaining a high transmission of the wavelengths of interest. A southward moving auroral surge with its strongest intensity eastward of the rocket trajectory is seen.

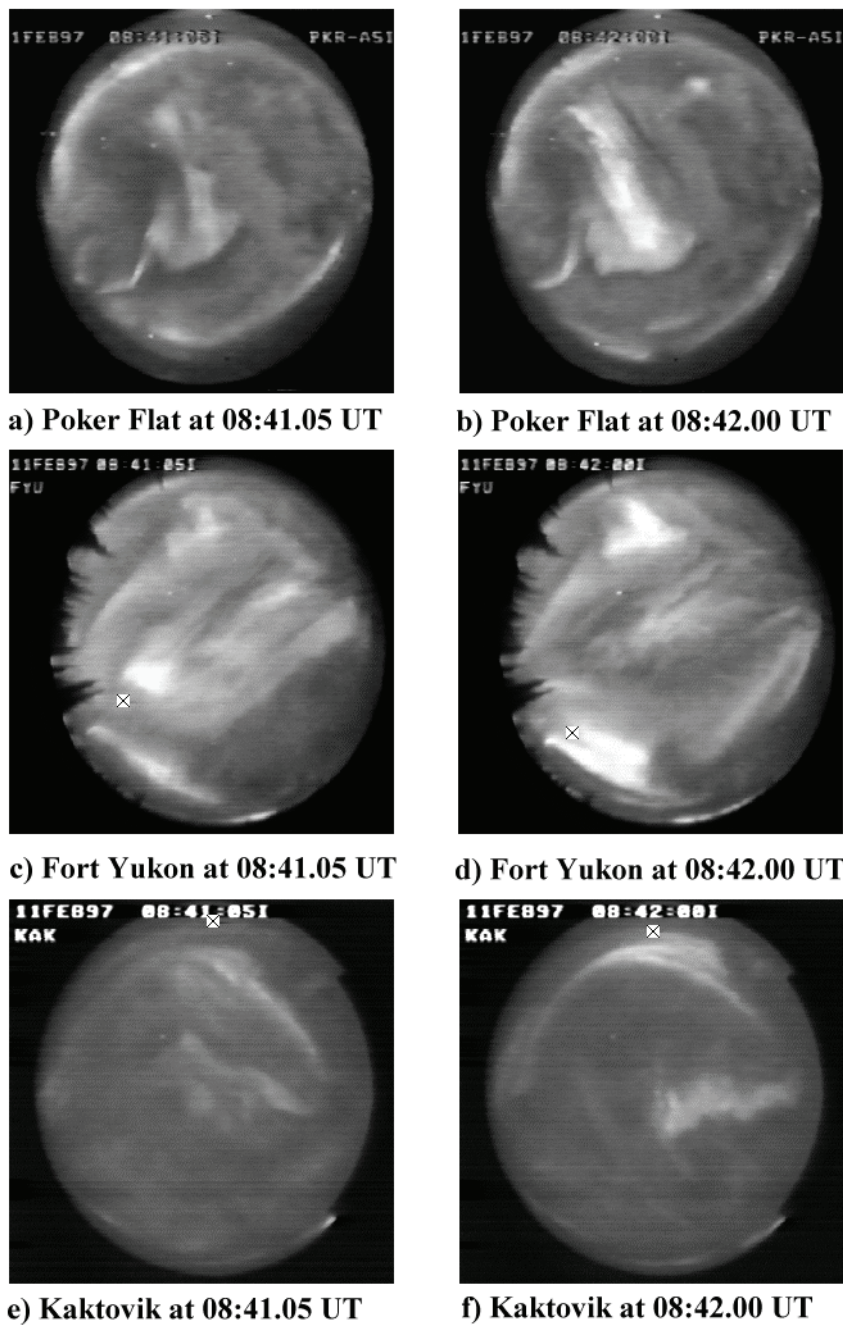


Fig. 1. All-Sky images taken on 11 February 1997 at 08:41:05 LT (a,c,e) and at 08:42:00 (b,d,f) Poker Flat, Fort Yukon and Barter Island - Kaktovik.

At around T+330 (T equals launch time) the payload cluster crossed a moderately active arc. In Figure 2 this event is shown from all three all-sky camera sites. The top of each image corresponds to geomagnetic south and the right side to magnetic west. The

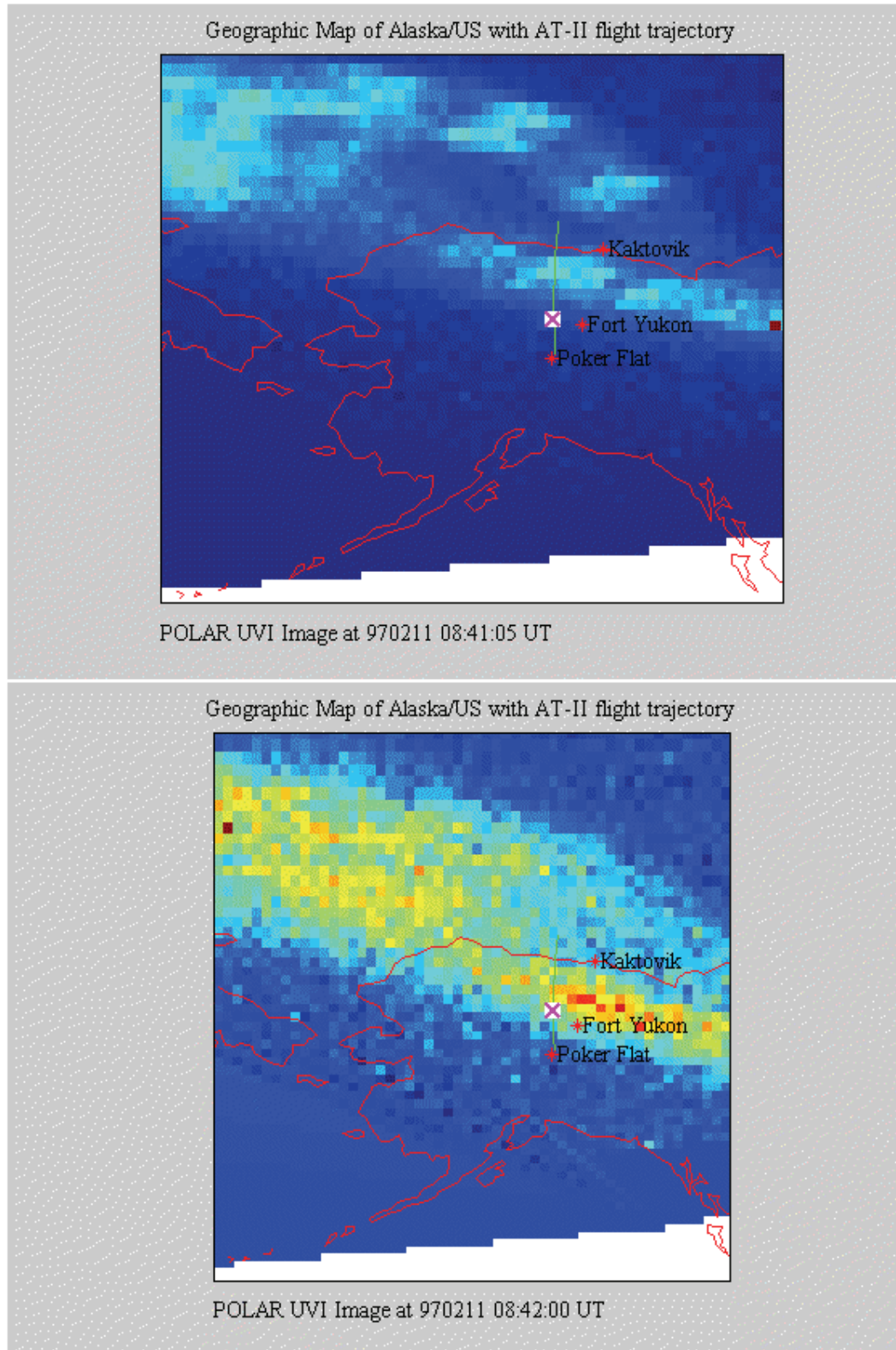


Fig. 2. Auroral structures above Alaska, taken by POLAR UV-Imager on February 11, 1997 at 08:41:05 LT (a) and at 08:42:00 (b).

images are sorted from lower to higher geographic latitude: Figure 2a, b, Poker Flat, Figure 2c, d, Fort Yukon and Figure 2e, f, Kaktovik. At all sites the all-sky cameras are oriented magnetically, e.g. at Kaktovik this means that the bottom of the images corresponds to a direction ~ 30 degrees east of geographic north. The payload cluster is marked in every image. Its position was determined by radar measurements and the altitude of the arc could be estimated by triangulation to be between 95 and 100 km.

3.2 *Satellite and ground based magnetic field measurements*

The geomagnetic background for the time of the Auroral Turbulence II sounding rocket experiment was measured by a network of satellite and ground based instruments. The time period around the rocket flight was characterised by disturbed geomagnetic conditions (daily $A_p=211.15$). The interplanetary magnetic field (IMF) and solar wind parameters were measured by the Wind satellite, which is operating between the Earth and the Sun at about 200 R_e from Earth. The IMF B_z component (Figure 3a, GSM coordinates) before 04:30 UT was small and positive (about 2nT). Around 04:30 UT of the IMF B_z -component makes a sudden turn to -5 nT. The solar wind velocity was about 450 km/sec, so this disturbance reached the magnetopause at about 05:15 UT (the delay time is in order of 45 minutes). The Geosynchronous Operational Environmental Satellites (GOES) are operating in a geostationary orbit at about 6.6 Earth radii close to the Earth's equatorial plane. For the time of the Auroral Turbulence II rocket experiment GOES 9 was at about 227° E, close to the field line of Poker Flat. In figure 3b the B_z component (GSM coordinates) measured by GOES 9 is shown. After 05 UT the magnetic field begins to decrease indicating tailward stretching of field lines and there are several negative spikes indicating a sequence of substorm onsets. After 05 UT, at the same time as the magnetic field begins to decrease at the GOES 9 and the meridian scanning photometer at Poker Flat (not shown) observes an increased precipitation, the Poker Flat magnetic H-component increases, (Figure 3c). At 08:15 UT, shortly before the rocket launch, a sharp decrease, about 700 nT, occurred at Poker Flat in the magnetic H-component indicating strong substorm activity.

3.3 *Rocket in-situ magnetic field measurement*

Figure 4 presents deflections of the measured magnetic field on the North and East payloads from the IGRF model. The measured magnetic field was scaled so that the minima in the model field and the measurements were the same. This provided quite a good correspondence between the measured and the model data. The upper panel presents the variation of the total magnetic field value (longitudinal deflection) after a square fit subtraction. Two panels in the middle present the transverse variations observed on the North and East payloads. The lower panel shows the variations of field-aligned currents derived from the measurements presented in the first three panels. All the presented data are sliding averages using a window of 6 seconds (corresponding to

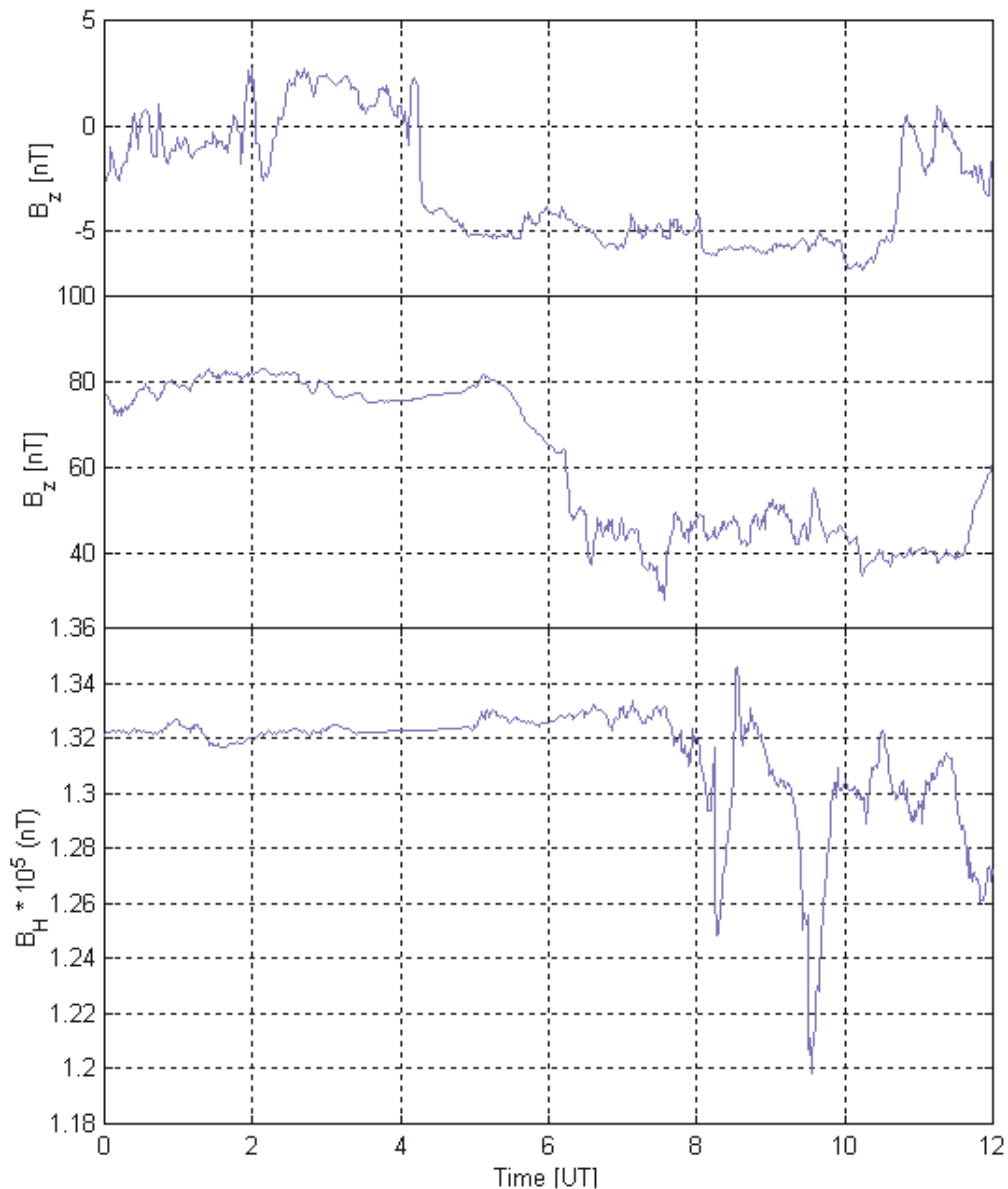


Fig. 3. a) Magnetic Z-component measured by the Wind satellite for 00:00 to 12:00 on 11 February 1997 is shown in the most upper graph. The Wind satellite measures the interplanetary magnetic field (IMF). b) The figure in the middle shows the variations of the near Earth magnetic field Z-component measured by the GOES 9 satellite on a geosynchronous orbit for the same time as in a). c) Finally the magnetic H-component at ground level were measured at Poker Flat Observatory.

6 km in terms of payload motion). On such a large scale all three payloads should observe essentially the same features, so the best resolved components in magnetic field-angular momentum plane (see Figure 4) are presented. The observations indicate the presence of a rather extended regime of upward field-aligned currents related to auroral arcs and downward field-aligned currents outside or between the arcs. The changes in the total field are smaller and more gradual than those of the transverse components, which indicates that the magnetic field variations are indeed caused by field aligned currents. The longitudinal component corresponds to transverse current effects. Transverse currents flow in the ionosphere, at about 100-150 km altitude, but

their effect at the rocket height is only minor as shown in Figure 3b. Gradients related to arcs and arc boundaries are indeed observed, especially the strongest one at T+400 s. The arc can be seen in Figure 1f close to the southern horizon, which is several minutes before the rocket crosses the arc. The good correspondence of the current signatures with the optical signatures is evident by comparing Figure 4 with Figures 1e and 1f. A strong arc was seen between T+380s -400 s, with a peak electron precipitation at around 390 s, and a void region following afterwards at T+405 s (private communication by K. Lynch, 1998).

Fig. 4. a) The total magnetic field value measured by the Aurora Turbulence II payload cluster was subtracted from the International Geomagnetic Reference Field model. The Auroral Turbulence II magnetic field measurements in the B,L-plane are shown for b) the north-south component North and for c) the east-west component East. The variations of field-aligned currents measured by North and East payloads are shown in d).

The region at around T+390 s indicates a strong downward current (*Marklund et al.*, 1998), while the adjacent void region corresponds to an upward current, as can be judged from the magnetic field gradients in the northern component (*Primdahl et al.*,

1984). This is consistent with the expected picture if the arc is extended from northwest to southeast. If we assume homogeneity along the arc we may derive how much the arc is deflected from the geographic east:

$$\tan a = (dBN / dx) / (dBE / dx). \quad (1)$$

With a ~ 40 to 45 degrees from the geographic east we find a general correspondence to the optical observations (Figures 2 e, f and 1 a, b). The difference of about 10 degrees between optical and magnetic observations could be due to inhomogeneities inside the arc. For the upward field-aligned current a value of 0.17 A/m was found. The downward field-aligned current equatorward of the arc is ~ 0.05 A/m, and poleward of the arc 0.12 A/m.

4. Discussion

Field-aligned current densities in and around a moderate active auroral arc structure were derived from the magnetic field measurements made in the Auroral Turbulence II sounding rocket experiment. The two main physical results of this study are:

- 1) A rather wide upward field-aligned current sheet was observed to be coincident with the optical arc.
- 2) The arc alignment as estimated from the optical observations (roughly 45° related to the geographic east-west) was found to agree with that interpreted from the magnetic field data (minim variance analysis). The upward arc current was balanced by return currents north and south of the arc.

Here we discuss these features in the context of substorm and aurora formation physics. The second point to be discussed is a relation of the observed phenomena to the large-scale magnetosphere-ionosphere current system.

4.1 On the physics of the arc

The observed auroral arcs occurred in the course of a substorm initiated by a southward turning of the IMF as measured by the Wind satellite magnetometer. The scenario of the substorm is of the same kind as that described by e.g. *Fairfield et al.*, (1981) and others. The disturbance reached the Earth's magnetosphere in about 45 minutes, which triggered the substorm. The growth phase starts by an enhancement of the convection electric field as the solar wind energy is transferred to the magnetosphere via reconnection between interplanetary and magnetospheric field lines. The tail lobe field strength increases, leading to a tailward stretching of field lines in the near-Earth tail (*Kaufmann*, 1987). Furthermore, a current sheet (TCS, down to 0.1 Re) forms just tailward of dipole-like field lines (6 - 15 Re). The increase of the crosstail current leads to a depression of the magnetic field closer to the Earth. In our case, the

depression was observed close to the midnight region by the GOES 9 satellite, which was located in a geosynchronous orbit. The increase of the crosstail current can be important for the triggering of the substorm (*Sergeev et al.*, 1990). Thus, magnetospheric processes driven by the reconnection at the day side and by the enhanced tail convection leads to the observed substorm onsets and the observed auroral arc structures.

A number of mechanisms have been proposed for the auroral arc formation (*Borovsky and Suszcynsky*, 1993). The mechanisms may be categorised into two main types according to the implied energy source. The energy may come from:

- 1) The large-scale convection electric field in the course of instability of the magnetosphere convection (e.g., *Trakhtengertz and Feldstein*, 1984).
- 2) Hot plasmashet plasma or, in other words, from the tail magnetic field in course of reconnection (section 4.3. in *Borovsky and Suszcynsky*, 1993) or interchange instability (e.g., *Miura et al.*, 1989).

Whereas the upward field-aligned current is a characteristic signature of auroral field line the location of the downward field-aligned return current may be variable.

Reconnection and magnetospheric convection instability lead to Earthward plasma flow in the neartail. The observed downward field-aligned current at the poleward edge of the arc may result from partial violation of the frozen-in condition for hot ions; the mechanism was described in (*Kozlovsky and Lyatsky*, 1999). In the case of interchange instability, plasma should move away from the Earth, so this mechanism faces some problems in explanation of the field-aligned current at the poleward edge of arc. Thus, the field-aligned current structure gives us a lot of information about magnetospheric process.

4.2 *Field-aligned currents in the auroral zone*

The assumptions about currents and their flow in and out along geomagnetic field lines from the Earth was made by *Birkeland* already 1908 and later continued by satellite measurements (e.g. *Gizler and Troshichev* (1978) and others). The currents derived from the AT-II magnetic field data are here compared with the optical data of the auroral arc structures observed during the rocket flight in the auroral oval close to the midnight sector. According to the POLAR UVI images the width of the auroral oval close to the rocket trajectory was between 64° - 76° N. Since *Iijima and Potemra*, (1976a,b) the large-scale distribution of the field-aligned currents has been known. In the midnight sector there is a characteristic triple current sheet signature before 24:00 MLT. Towards the dawn this triple structure merges into a double current sheet, which has been seen during the Auroral Turbulence II rocket experiment. The observed magnetically east-westward orientation of the auroral arc is consistent with the observations of field-aligned current sheets. The latitudinal distribution of the amplitudes and directions of the region of field-aligned currents were found for the

Auroral Turbulence rocket experiment to be in agreement with earlier studies by, e.g. *Saflekos et al.*, (1982) and *Robinson et al.*, (1981). The studied auroral arc structure is located at the edge of the upward region 2 (*Iijma and Potemra*, 1976a,b) current sheet. The downward field-aligned current sheet polewards may be connected with ionospheric plasma cavities, which are observed frequently poleward of auroral arcs (*Doe et al.*, 1993).

The results show a very consistent picture with upward field-aligned currents within the arc structures and downward field-aligned currents within regions void of optical emission. The field-aligned current densities for the midnight sector, in- and outside the arc are consistent with earlier observations (*Gizler et al.*, 1979, *Saflekos et al.*, 1982).

Acknowledgement

We would like to thank Prof. Dr. J. Kangas and Dr. A. Kozlovsky for helpful advises and discussions during the preparation of this study. Without the data provided by the POLAR UV-imager Team and Prof. Dr. T. Hallinan and the magnetometer data provided by J. Olson of the Geophysical Institute, University of Alaska this work would have not been possible. Especially we would like to thank T. Oneager at NOAA SEC and CDAWeb for providing the GOES 8 and GOES 9 satellite data. The magnetic experiment was supported by the Academy of Finland.

References

- Birkeland, K., 1908. *The Norwegian Aurora Polaris Expedition 1902-1903, Vol 1*, Christiania, Norway.
- Borovsky, J. and D. Suszcynsky, 1993. Optical measurements of the fine structure of auroral arcs. *Geophysical Monograph*, **25**.
- Doe, R.A., M. Mendillo, J.F. Vickrey, L.J. Zanetti, R.W. Eastes, 1993. Observations of nightside auroral cavities. *J. Geophys. Res.*, **98**, A1, 293-310.
- Evans, J., N. Maynard, J. Troim, T. Jacobsen and A. Egeland, 1977. Auroral Vector electric field and particle comparisons: 2. Electrodynamics of an Arc. *J. Geophys. Res.*, **82**, 16, 2235-2249.
- Fairfield, D.H., R.P. Lepping, E.W. Hones, Jr., S.J. Blame and J.R. Asbridge, 1981. Simultaneous measurements of magnetotail dynamics by IMP spacecraft. *J. Geophys. Res.*, **86**, 1396-1414.
- Gizler, V. and O. Troshichev, 1978. Longitudinal electric currents and polar magnetic disturbances. *Geomagnitnye Issledovaniia*, **23**, 24 -51.
- Gizler, V., V. Semenov and O. Troshichev, 1979. Electric fields and currents in the ionosphere generated by field-aligned currents observed by Triad. *Planet. Space Sci.*, **27**, 223-231.

- Iijima, T. and T.A. Potemra, 1976a. The amplitude of field-aligned currents at northern high latitudes observed by TRIAD. *J. Geophys. Res.*, **81**, 2165.
- Iijima, T. and T.A. Potemra, 1976b. Field-aligned currents in the dayside cusp observed by TRIAD. *J. Geophys. Res.*, **81**, 5971.
- Johnstone, A. and T. Davis, 1974. Low-altitude acceleration of auroral electrons during breakup observed by a mother-daughter rocket. *J. Geophys. Res.*, **79**, 10, 1416-1425.
- Kaufmann, R.L., 1987. Substorm currents: growth phase and onset. *J. Geophys. Res.*, **92**, 7472-7489.
- Kozlovsky, A. and W. Lyatsky, 1999. Finite Larmor radius convection instability in the near-Earth plasma sheet. *J. Geophys. Res.*, **104**, A2, 2243.
- Lühr, H., 1992. In situ ionospheric current measurements during ROSE rocket flights: evidence for tilted current layers. *J. Atmospheric and Terrestrial Phys.*, **54**, 6, 725-731.
- Marklund, G., I. Sandahl and H. Opgenoorth, 1982. A study of the dynamics of a discrete auroral arc. *Planet. Space Sci.*, **30**, 179-197.
- Marklund, G., 1984. Auroral arc classification scheme based on the observed arc-associated electric field pattern, *Planet. Space Sci.*, **32**, 2, 193-211.
- Marklund, G., T. Karlsson, L. Blomberg, P.-A. Lindqvist, C.-G. Fälthammar, M. Johnson, J. Murphree, L. Andersson, L. Eliasson, H. Opgenoorth and L. Zanetti, 1998. Observations of the electric field fine structure associated with the westward travelling surge and large-scale auroral spirals. *J. Geophys. Res.*, **103**, A3, 4125-4144.
- Miura, A., S. Ohtani and T. Tamao, 1989. Ballooning instability and structure of diamagnetic hydromagnetic waves in a model magnetosphere. *J. Geophys. Res.*, **94**, 15,231-15,242.
- Robinson, R.M., E.A. Bering, R.R. Vondrak, H.R. Anderson and P.A. Cloutier, 1981. Simultaneous rocket and radar measurements of currents in an auroral arc. *J. Geophys. Res.*, **86**, A9, 7703-7717.
- Primdahl, F., J. Walker, F. Spangslev, J. Olesen, U. Fahlson and E. Ungstrup, 1979. Sunlit cleft and polar cap ionospheric currents determined from rocket-borne magnetic field, plasma, and electric field observations. *J. Geophys. Res.*, **84**, A11, 6458-6470.
- Primdahl, F., A. Bahnsen, M. Ejiri, P. Hoeg, G. Marklund, B. Mæhlum, J. Olesen, E. Ungstrup and L. Zanetti, 1984. Rocket-borne and groundbased observations of coincident field-aligned currents, electron beams, and plasma density enhancements in the afternoon auroral oval. *Planet. Space Sci.*, **32**, 5, 561-583.
- Primdahl, F., 1994. Digital detection of the flux-gate sensor output signal. *Meas. Sci. Technol.*, **5**, 359-362.

- Saflekos, N., R. Sheehan and R. Carovilland, 1982. Global nature of field-aligned currents and their relation to auroral phenomena. *Rev. Geophys. and Space Phys.*, **20**, 3, 709-734.
- Sergeev, V.A., P. Tanskanen, K. Mursula, A. Korth and R.C. Elphic, 1990. Current sheet thickness in the near-earth plasma sheet during substorm growth phase. *J. Geophys. Res.*, **95**, 3819-3828.
- Trakhtengertz, V.Yu. and A.Ya. Feldstein, 1984. Quiet auroral arcs: Ionosphere effect of magnetospheric convection stratification. *Planet. Space Sci.*, **32**, 127-134.
- Torr, M., 1995. A far ultraviolet imager for the International solar-terrestrial physics mission. *Space Sci.Rev.*, **71**, 329-383.
- Zukic, M., 1993. Filters for the international solar terrestrial physics mission. *Opt. Eng.*, **32**, 3069.